Available online at **www.joac.info**

ISSN: 2278-1862

Journal of Applicable Chemistry

2021, 10 (6): 838-852

(International Peer Reviewed Journal)

Review

A Review of *Gloriosa Superba Linn* Corrosion Prevention of Mild Steel in HCl Media

P. R. Sivakumar*

Department of Chemistry, Adithya Institute of Technology, Coimbatore, Tamil Nadu, **INDIA**

Email: shivarashee@gmail.com

Accepted on 16th November, 2021

ABSTRACT

The corrosion inhibition and adsorption behaviour of alcoholic extracts of plants, namely Gloriosa Superba Linn on mild steel surfaces in 1N HCl solution were explored by mass loss with varying contact times, different temperatures, and electrochemical impedance and Tafel tests. According to the polarisation technique, the plant extract acted as a mixed type inhibitor, primarily controlling the anodic reaction. The adsorption of inhibitor caused a structural change at the electrode solution interface, resulting in mild steel dissolving being controlled by the C_{dl} mechanism, according to the EIS analysis. SEM investigation has established the nature of the protective coating produced on the MS surface. The surface coverage numbers were graphed in order to find an adsorption isotherm that suited the data. In the acid media, the plant extract proved to be an effective natural corrosion inhibitor.

Highlights

- The GSL medicinal plants extract acts as an inhibitor for corrosion of mild steel in 1N HCl solution.
- A good agreement was observed between the results of weight loss and electrochemical methods
- The GSL plants extracts act as a mixed type inhibitor on the metal surface.
- The plant materials contain proteins, tannin, alkaloids, and terpenoids and so forth. These compounds are potential acid corrosion inhibitor for many metals.
- The nature of the protective layer formed on the metal surface has been characterized by Scanning Electron Microscopy (SEM).
- The plant extract obey Temkin adsorption isotherm.
- The temperature studies revealed decrease inhibition efficiency with increase temperature which suggests physisorption.

Keywords: Metals, Corrosion test, EIS, SEM.

INTRODUCTION

Inhibitors are one of the most practical ways to prevent metals against corrosion, especially in acidic environments. The objective of research in the field of green or eco-friendly corrosion inhibitors in

the twenty-first century has been to use affordable, effective compounds with little or no environmental impact. Plant extract is inexpensive and environmentally friendly, and it may be produced by a simple extraction procedure [**1-9**]. It is also biodegradable. The fundamental benefit of employing plant extract as a corrosion inhibitor is that it is both cost-effective and environmentally friendly. Until date, various plant extracts have been researched as efficient steel corrosion inhibitors in inorganic acids such as HCl, H_2SO_4, and H_3PO_4 and plant leaves extract has been reported as an effective mild steel corrosion inhibitor in HCl [**10-20**].Obviously, given the wide variety of plant extracts available, information on the use of whole plant extract as a mild steel corrosion inhibitor in HCl acid is limited. Furthermore, to the best of our knowledge, the literature on plant extract as a mild steel corrosion inhibitor in 1N HCl acid solution is essentially non-existent [**21-24**]. Much research has been done in our lab to see if GSL extract may prevent mild steel from corroding in an acidic environment. The key argument for choosing GSL is that complete parts are plentiful resources with quick renewal and continuous usage, as well as being nonpoisonous and therapeutic [**25-30**]. Meanwhile, the variation in inhibition performance across GSL is explored in order to obtain insight into the role of main components in corrosion inhibition and the inhibitive process. It is intended to offer helpful information on the inhibitive impact of GSL plant extract in 1N HCl acid solution for mild steel.

MATERIALS AND METHODS

Preparation of mild steel specimen: Mild steel strips were mechanically cut into strips of size 4 cm x 2 cm x 0.1 cm containing the composition of C- 0.030 %, Mn- 0.169 %, Si- 0.015 %, P- 0.031 %, S - 0.029 %, Cr- 0.029 %, Ni- 0.030 %, Mb- 0.016 %, Cu- 0.017 % and the remainder Fe and provided with a hole of uniform diameter to facilitate suspension of the strips in the test solution for weight loss method. Mild steel strips with the same composition but a $1cm^2$ exposed areas were employed for electrochemical investigations. Mild steel strips were polished with 400, 600, 800, 1000, and 1200 grit emery paper, then degreased with acetone and cleaned with deionized water before being kept in the desiccator. Four digital electronic balances were used to get an accurate weight of the metal (shimadzu ay 220 model).

Preparation of the plant extract: *Gloriosa Superba* leaves, stems, tubers, and flowers were chopped into small pieces, dried at room temperature, and pulverized into powder. 10g of each powder was refluxed in 150 mL of distilled water overnight. The refluxed solution was then thoroughly filtered, and the filtrate volume was increased to 250 mL using double distilled water as the stock solution, with the stock solution's concentration reported in terms of v/v.

Weight loss method: Glass hooks and rods were used to immerse mild steel specimens in 200 mL of 1N HCl solution without and with varied doses of inhibitors for predefined time duration (24 h) at room temperature. A four-digit electronic balance was used to determine the weights of the specimens before and after immersion (shimadzu ay 220 model). The corrosion rate was computed using the following relationship based on the weight loss observations.

$$CR\,(mmpy) = \frac{K \times \text{Weight Loss}}{D \times A \times t\ (\text{in hours})} \quad \ldots(1)$$

Where, K = 8.76×10^4 (constant), D is density in gm/cm^3 (7.86), W is weight loss in grams and A is area in cm^2.

The inhibition efficiency (%) was calculated using equation (2)

$$IE\,\% = \frac{W_0 - W_i}{W_0} \times 100 \quad \ldots(2)$$

Where, W_0 and W_i are the weight loss in the absence and presence of the inhibitor respectively.

FTIR measurements: A Bruker ALPHA 8400 S spectrophotometer was used to record FTIR spectra. The film was carefully removed, completely mixed with KBr and formed into pellets, and FTIR spectra were taken.

Pontetiodynamic polarization methods: Using a CHI660E electrochemical analyzer, potentio-dynamic polarisation experiments were performed. Polarization measurements were conducted to determine the corrosion current and potential at the Tafel slope. Experiments were conducted in a three-electrode cell assembly with a mild steel specimen of 1 cm^2 area exposed and the remainder coated with red lacquer as working electrode, a rectangle Platinum foil as counter electrode, and a saturated calomel electrode as standard reference electrode. To achieve the steady state open circuit potential, each experiment was given a 15-minute time interval. At a sweep rate of 1 mV per second, the polarisation was moved from a cathodic potential of -800 mV (vs SCE) to an anodic potential of -200 mV (vs SCE). Tafel slopes, corrosion potential, and corrosion current were calculated using the polarization curves as a starting point. The formula for calculating inhibitor efficiency was:

$$IE\ \% = \frac{I_{Corr} - I_{*Corr}}{I_{Corr}} \times 100 \qquad \ldots (3)$$

Where I_{corr} and I_{*corr} are corrosion current in the absence and present of inhibitors.

Electrochemical impedance method: The CHI660E electrochemical analyzer was also used to test electrochemical AC-Impedance. Experiments were conducted in a three-electrode cell setup similar to that utilised in potentiodynamic polarisation investigations. A 10 mV sine wave was superimposed on the steady state open circuit voltage. At frequencies ranging from 100 KHz to 10 MHz, the real component (Z') and the imaginary part (Z") were measured. Z' vs Z" was plotted. The charge transfer resistance (R_{ct}) was determined from the plot, and the double layer capacitance (C_{dl}) was derived using the following formula:

$$C_{dl} = \frac{1}{2\pi} f_{max} R_{ct} \qquad \ldots (4)$$

Where R_{ct} is charge transfer resistance, and C_{dl} is double layer capacitance. The experiments were carried out in the absence and presence of different concentration of inhibitor.

$$IE\% = \frac{R_{ct} - R^0_{ct}}{R} \times 100 \qquad \ldots (5)$$

Where, R_{ct} and R^0_{ct} are the charge transfer resistance values in the inhibited and uninhibited solution respectively.

Phytochemical analysis: The principal secondary metabolites such as alkaloids, flavonoids, glycosides, proteins, phenolic compounds, saponins, starch, steroids, tannins, and terpenoids were identified using phytochemical screening employing frequently used precipitation and colouring processes.

Scanning electron microscopy: The mild steel specimen was removed after one day of immersion in blank and inhibitor solutions, cleaned with double distilled water, dried, and examined under a scanning electron microscope for surface morphology. A (JEOL) computer controlled scanning electron microscope was used to analyze the surface morphology of mild steel.

Effect of immersion time: The mild steel coupons were submerged in 100 mL of the test solution without and with various concentrations of GSL extract for 1 h, 3 h, 5 h, 7 h and 12 h at room

temperature. The weight of the coupons was evaluated before and after immersion. The mild steel's inhibition efficiency was determined.

Effect of temperature: The polished and pre-weighed specimens were suspended in 100 mL of the test solution for 1 h at temperatures ranging from 303 to 323 K using water thermostats, with and without the addition of various concentrations of GSL extract. After 1 hour in the test solution, the specimens were removed and rinsed with distilled water before being dried and weighed. Weight loss was used to determine the inhibitory efficiency.

RESULTS AND DISCUSSION

Gravimetric method: The most widely utilized way of main calculation is the weight loss procedure. In this work, changed mild steel samples were immersed in a 1N HCl solution containing acid for 24 h in the absence and presence of different plant extract concentrations. Table 1 shows the corrosion characteristics of the alcoholic extract of GSL plants obtained using the weight loss technique. The data revealed that when inhibitor concentrations were steadily raised, weight loss and corrosion rate reduced, and inhibition efficiency was determined to be greater (94.12 percent for leaves) at 20 v/v. The results show that adding inhibitors to GSL extract increases its inhibition efficiency on mild steel surfaces in 1N HCl medium via adsorption and protects against corrosion. The results showed that GSL leaves > stem> tubers > flowers at the optimal dose (20 v/v) of all four inhibitors.

Table 1. Percentage of corrosion rate (CR) and inhibition efficiency (IE %) at different concentration of inhibitor in 1N HCl medium.

Alcoholic extract of GSL plants				
Parts of plant	**Conc. of the extract (v/v)**	**Weight loss (g)**	**Corrosion rate (mmpy)**	**IE (%)**
Gloriosa Superba Linn **leaves**	Blank	0.1107	34.258	-
	5	0.0011	0.618	64.12
	10	0.0017	0.526	79.64
	15	0.0013	0.454	84.02
	20	0.0015	0.370	94.12
Gloriosa Superba Linn **Stems**	Blank	0.0445	25.830	-
	5	0.0046	2.017	60.54
	10	0.0040	1.918	64.20
	15	0.0001	0.916	79.52
	20	0.0035	0.431	92.13
Gloriosa Superba Linn **flowers**	Blank	0.0350	21.112	-
	5	0.0083	3.170	66.66
	10	0.0052	0.456	69.45
	15	0.0035	0.290	72.22
	20	0.0030	0.121	89.08
Gloriosa Superba Linn **tubers**	Blank	0.0849	34.210	-
	5	0.0089	4.106	31.15
	10	0.0013	2.182	52.17
	15	0.0120	2.065	73.48
	20	0.0234	1.920	90.35

FTIR Measurement: As a result of the FTIR analysis, the protective coating on the anodic sites of the metal surface is composed of Fe^{2+} - an organic element. The FTIR spectra of several sections of the *Gloriosa Superba* Linn plants, such as leaves, stems, tubers, and flower extract, are presented in figure 1. *Gloriosa Superba* Linn has bands (leaves, stems, flowers, and tubers) that correspond to (hydroxyl group) 3301, 3272, 3396, 3170 cm^{-1}, respectively. At 1645 cm^{-1}, there is a strong peak that corresponds to (carbonyl group).C-H aliphatic stretching is detected at frequencies of 2921, 2923,

2923, and 2967 cm^{-1} in leaves, stems, flowers, and tubers, respectively. The existence of an aromatic ring is indicated by the absorbance at 1597 and 1648 cm^{-1}, as well as many bands between 1328 and 1040 cm^{-1}. According to the findings, medicinal plants include nitrogen and oxygen (O-H, C=O, C-O) in diverse functional groups and aromatic rings, making this extract suitable for use as an inhibitor. These results also confirm that the FTIR spectra support the fact that the corrosion inhibition of GSL plants of alcoholic extract on mild steel in 1N HCl solution may be adsorption of active molecules in the inhibitor and the surface of metal [**31, 32**].

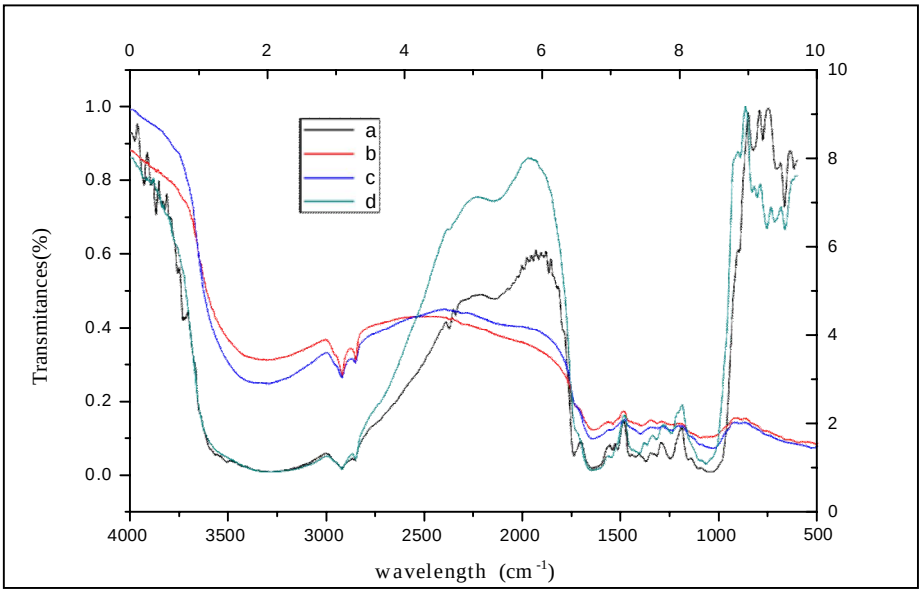

Figure 1. FTIR Spectra of *Gloriosa superba*leaves, stems, flowers and tubers Extracts.

Potentiodynamic polarization studies: Table 2 shows the Tafel parameters for mild steel in the absence and presence of an inhibitor concentration of GSL extract in 1N HCl, as well as the polarization curve as shown in figure 2. The addition of GSL has no effect on the values of Ecorr, but it does impact both anodic dissolution of mild steel and cathodic reduction reaction, suggesting that the composite might be categorized as a mixed type inhibitor. The corrosion current density (Icorr) decreases with increasing inhibitor concentrations, as seen in the table. The greatest inhibition efficiency reported at higher inhibitor concentrations indicates that more inhibitor molecules are deposited on the metal surface, providing more surface coverage for MS active regions where direct attack occurs and corrosion attack migrates. The findings show that when the content of alcoholic extract increases, the Ecorr values change more positively [**33**]. The corrosion current density, on the other hand is significantly reduced when the corrosion inhibitor is added. *Gloriosa Superba Linn* flower extract had a maximal inhibitory efficacy of 90.67 percent at 15 v/v when the concentration of the plant extract was raised.

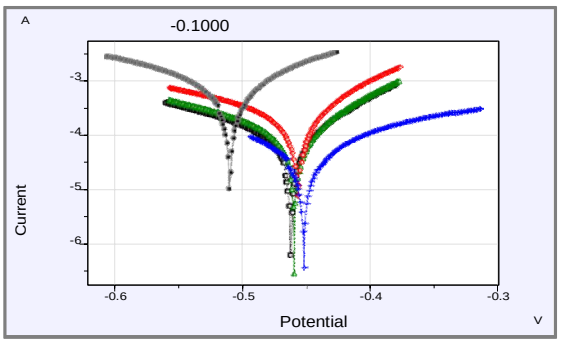

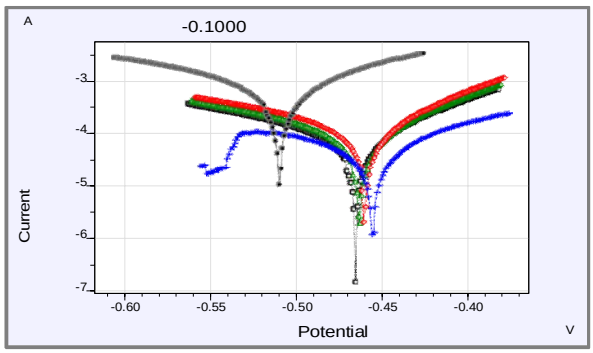

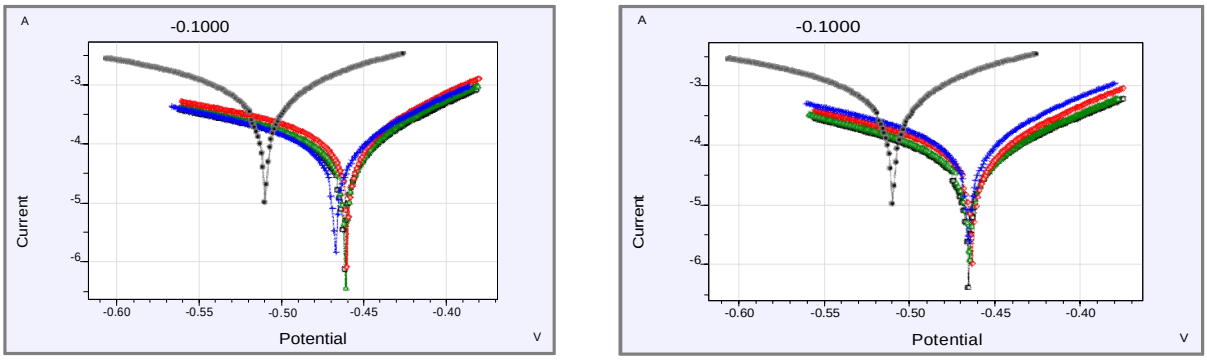

Figure 2. Potentiodynamic polarization (Tafel) curves for mild steel in 1N HCl solution in the absence and presence of different concentration of Gloriosa Superba extracts of (a) leaves (b) barks (c) flowers (d) tubers.

Table 2. Polarization measurement and calculated values of IE (%) at different concentration of GSL extract

Alcoholic extract of GSL plant						
Parts of *GSL* plant	**Conc. v/v**	**E_{cor} / mV/ SCE r**	**I_{corr}/ mA/cm^2**	**b_c mV/dec**	**b_amV/dec**	**IE (%)**
	Blank	-0.477	$1.5x10^{-3}$	128	87	*
	5	-0.463	$0.9x10^{-4}$	138	72	40.02
GS Linn	10	-0.471	$0.7x10^{-5}$	138	72	53.33
leaves	15	-0.475	$0.4x10^{-5}$	135	66	73.49
	20	-0.469	$0.7x10^{-6}$	147	65	80.97
	Blank	-0.477	$1.5x10^{-3}$	128	87	*
	5	-0.445	$0.9x10^{-5}$	134	67	76.95
GS Linn	10	-0.467	$0.3x10^{-4}$	142	67	84.65
flowers	15	-0.489	$0.6x10^{-4}$	139	66	90.67
	20	-0.478	$0.6x10^{-4}$	139	66	90.67
	Blank	-0.477	$1.5x10^{-3}$	128	87	*
	5	-0.477	$0.9x10^{-6}$	150	90	74.32
GS Linn	10	-0.486	$0.6x10^{-6}$	143	100	60.00
stems	15	-0.472	$0.7x10^{-6}$	154	90	73.33
	20	-0.472	$0.8x10^{-6}$	154	89	73.33
	Blank	-0.477	$1.5x10^{-3}$	128	87	*
	5	-0.483	$1.6x10^{-6}$	87	125	60.89
GS Linn	10	-0.474	$1.2x10^{-6}$	137	96	75.98
tubers	15	-0.462	$2.6x10^{-6}$	146	88	53.78
	20	-0.469	$2.6x10^{-6}$	133	89	53.78

Electrochemical impedance studies: Impedance spectroscopy is a straightforward and repeatable method. Figure 3 depicts the immersion of a mild steel sample in an acid media containing an alcoholic extract (without and with) of GSL extract at room temperature. After 20 min, a Nyquist plot was generated across a wide frequency range. Figure 3 displays Nyquist plots of several components of *Gloriosa Superba* Linn plants at varying concentrations, including leaves, stems, tubers, and flowers. Table 3 shows the various corrosion parameters calculated from EIS measurements. The impedance spectra show a single semicircle, and the diameter of the semicircle increases as the inhibitor concentration increases, indicating that the charge-transfer process primarily controls mild steel surface corrosion by delaying the electron transfer reaction and forming a strong protective film. The data reveal that as the inhibitor concentration rises (forming a protective layer), the Rct rises as well, indicating that the inhibitor efficiency rises as well. With minor variations, the results obtained from the polarisation area in acid-alcoholic solution were in good agreement with those obtained from the EIS.

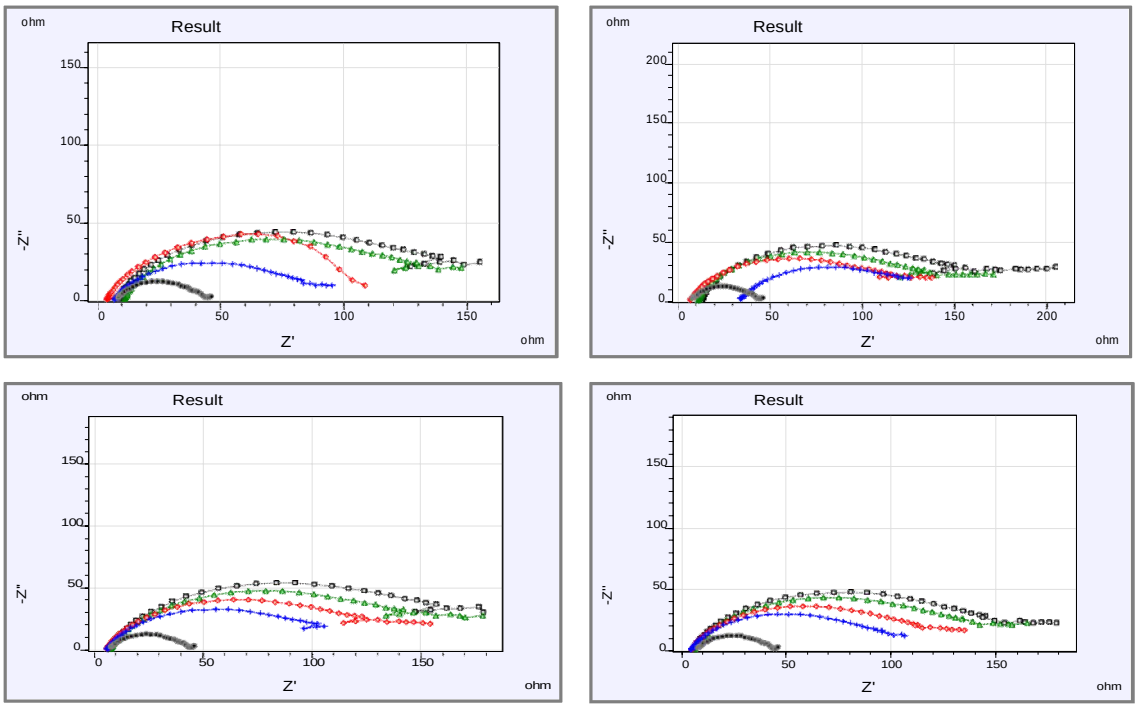

Figure 3. Nyquist plots for mild steel in 1N HCl acid solution without and with presence of different concentration of *Gloriosa superba*extract of (a) leaves (b) bark (c) flowers (d) tubers.

Table 3. EIS parameter for MS in 1N HCl acid solution without and with the varied concentration of GSL plant extract

Alcoholic extract of GSL plants				
Parts of *GSL* plant	**Concentraion (v/v)**	**R_{ct} (ohm cm^2)**	**C_{dl} (µF/cm^2)**	**IE (%)**
	Blank	20.70	$1.0x10^{-5}$	*
	5	33.09	$8.2x10^{-5}$	37.44
Gloriosa Superba Linn **leaves**	10	35.42	$6.4x10^{-5}$	41.55
	15	46.85	$7.2x10^{-5}$	55.81
	20	53.38	$3.3x10^{-6}$	61.22
	Blank	20.70	$1.0x10^{-5}$	*
	5	29.14	$5.9x10^{-7}$	28.96
Gloriosa Superba Linn **flowers**	10	42.90	$6.5x10^{-7}$	52.91
	15	48.67	$1.3 x10^{-7}$	57.46
	20	49.80	$1.8x10^{-7}$	57.83
	Blank	20.70	$1.0x10^{-5}$	*
	5	28.91	$1.1 x10^{-7}$	28.39
Gloriosa Superba Linn **Stems**	10	52.93	$4.3x10^{-6}$	60.89
	15	82.40	$6.1x10^{-6}$	74.87
	20	60.87	$4.9x10^{-8}$	65.99
	Blank	20.70	$1.0x10^{-5}$	*
	5	38.27	$1.9x10^{-5}$	45.91
Gloriosa SuperbaLinn **tubers**	10	47.57	$3.4 x10^{-7}$	56.48
	15	58.89	$5.8x10^{-7}$	64.84
	20	72.12	$6.8x10^{-7}$	71.29

Surface examination studies and EDAX Measurement: Scanning Electron Microscopy (SEM) was used to examine the morphologies of MS submerged in blank 1N HCl and with the optimal inhibitor

concentration for 24 h in figure 4 (a, b, c, d and e). According to SEM pictures, the plant extract that was adsorbed on the metal surface reduced corrosion attack on the metal surface. In 1N hydrochloric acid media, GSL plants extract acts as an effective green inhibitor.

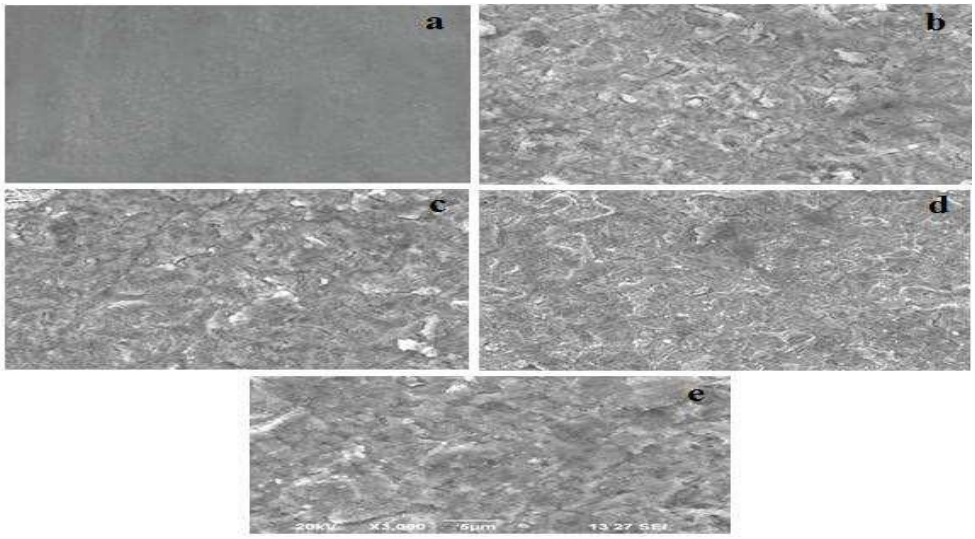

Figure 4. SEM image of the surface of mild steel after immersion for 24 h in 1N HCl solution (a) blank and in the presence of optimum concentration of the plant extracts from (b) Stem, (c) Leaves, (d) Flowers and (e) Tubers.

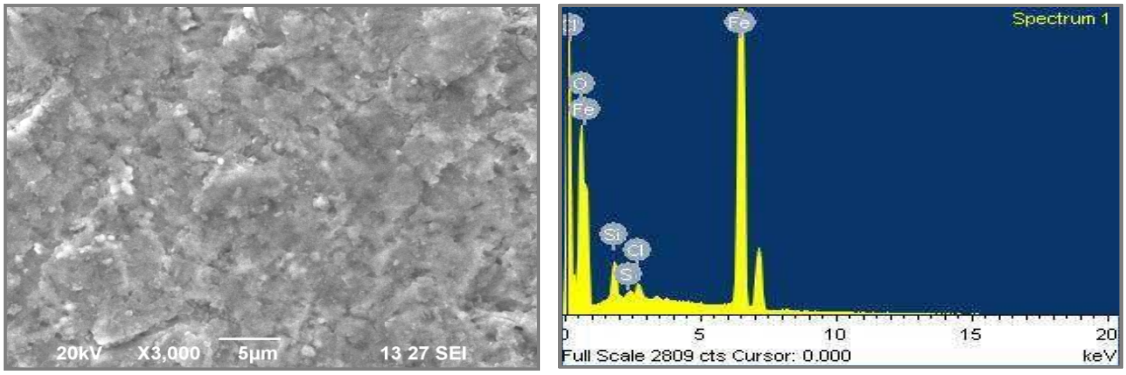

Figure 5. SEM image of the surface of mild steel and EDAX.

The purpose of this section was to validate that a protective surface coating of inhibitor is generated on the electrode surface based on the findings of chemical and electrochemical measurements. Figure 5 shows the associated energy dispersive EDAX profile analysis. To establish which elements of extract components were exposed to acid solution and inhibitor treatment, the EDAX survey spectra were employed. The presence of the EDAX spectra in the case of the sample subjected to the extract might be attributed to organic molecules adsorbing on the mild steel surface.The Fe peaks are significantly suppressed in comparison to samples generated in 1N HCl solution, as shown in the figure, and this suppression increases when the extract concentration and immersion duration are increased. The Fe lines are suppressed due to the extract film that lies on top of them. These findings corroborate those obtained from polarisation measurements, indicating that a surface coating slowed metal breakdown and therefore the hydrogen evolution event. This surface coating also reduces the rate of mild steel corrosion by increasing charge transfer resistance during anodic dissolution.

Influence of Time: The pretreatment specimens were submerged completely and individually in 100 mL of 1N HCl at 27°C. Table 4 shows the inhibitory efficacy of GSL alcoholic extract on mild steel

as a function of time. As a result, more adsorption occurs on the mild steel surface, the IE rises as immersion duration increases, and the inhibitory effects of the GSL extract are rather excellent in the examined circumstance. Uninhibited MS coupons were shown to be the least protective, as predicted. Since GSL is a well-known substance, it has been widely employed as a corrosion inhibitor.

Table 4. Inhibition efficiency of alcoholic extract of GSL plants at various immersion time

Parts of GSL plant	Conc. extract (v/v)	Inhibition efficiency (%)						
		1h	3h	5h	7h	9h	12h	3 days
	Blank	-	-	-	-	-	-	-
Gloriosa Superba linn **leaves**	5	27.09	40.35	54.32	63.79	66.76	71.53	47.90
	10	29.34	47.67	60.79	66.67	68.10	78.10	46.78
	15	40.35	55.89	64.09	75.77	77.96	80.72	45.87
	20	53.49	66.21	73.51	81.89	80.78	93.92	45.87
Gloriosa Superba linn **stems**	5	23.56	35.90	49.57	75.86	76.36	79.06	58.00
	10	27.89	41.43	62.12	78.03	80.84	89.72	57.35
	15	38.07	49.67	64.75	79.56	88.90	94.17	55.90
	20	53.25	59.72	70.09	89.90	93.05	96.75	55.90
Gloriosa Superba linn **flowers**	5	40.54	50.23	61.23	76.98	88.45	89.39	47.89
	10	53.90	59.46	66.44	78.54	89.04	90.07	40.55
	15	63.72	69.03	70.96	87.02	91.90	93.56	33.90
	20	80.43	88.34	89.37	94.76	92.09	97.49	33.89
Gloriosa Superba linn **tubers**	5	49.34	58.38	60.11	71.34	79.56	88.88	41.20
	10	56.90	70.17	72.54	76.09	84.00	89.45	37.39
	15	66.75	72.64	78.96	85.23	88.73	90.92	28.90
	20	88.80	89.97	96.37	97.17	97.43	97.52	28.87

Influence of temperature: Gravimetric tests were conducted at various temperatures (303-323K) in the absence and presence of various concentrations of the inhibitor during 3 h of immersion to determine the influence of temperature on corrosion and corrosion inhibition. Table 5 summaries the findings.

Table 5. The percentage inhibition efficiency of *Gloriosa Superba Linn* plants at various temperatures

Alcoholic extract of GSL plants				
Parts of (GSL) plant	Conc. of the extract (v/v)	IE (%)		
		303K	313K	323K
	Blank	-	-	-
Gloriosa Superba Linn **leaves**	5	59.48	60.24	46.48
	10	69.59	77.54	55.36
	15	81.36	83.74	68.04
	20	91.02	87.22	73.66
Gloriosa Superba Linn **stem**	5	65.71	56.58	59.58
	10	73.89	62.24	64.86
	15	77.48	74.41	69.24
	20	80.45	77.13	75.50
Gloriosa Superba Linn **flowers**	5	66.12	59.90	47.41
	10	67.90	61.55	60.55
	15	73.65	66.86	66.27
	20	74.97	72.12	79.80
Gloriosa Superba Linn **tubers**	5	39.25	50.29	40.02
	10	64.48	60.73	54.82
	15	71.49	66.69	68.18
	20	77.59	74.78	73.10

Cyclic Voltammetry Measurement: Cyclic voltammetry method was carried out CHI-660 Eletrochemical Analyzer. The experiments were carried out in conventional three electrode cell assembly as that for cyclic voltammetry.

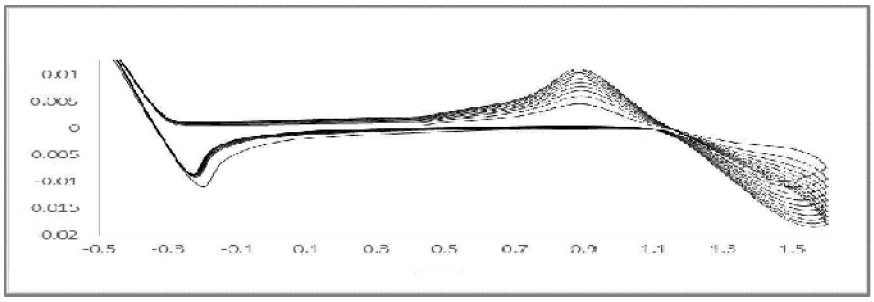

Figure 6. Cyclic voltammetry of mild steel in alcoholic extract.

The mild steel specimens' cyclic voltammograms in 1N HCl containing varied concentrations of plant extract are presented in Figure 6. In the blank solution, there is one anodic and one cathodic current peak. We can see the initial oxidation peak in the CV plots when anodic dissolution of mild steel happens through reaction. As a result, the reaction of mild steel to soluble Fe^{2+} is represented by the second oxidation peak. On the one hand, the mild steel corrosion product can be partially reduced in reserve sweep, as mentioned previously. The increase in film layer, on the other hand, would slow down the corrosion process to some amount. An anodic current hump appears in CV plots on the reverse sweep at about +1.4 V due to competition between dissolution and adsorption of the film on mild steel. Because the sweep rate is sufficiently high, the rate of film dissolution is hardly compensated by the precipitation of corrosion products, and the anodic current hump becomes clear. Meanwhile, when the inhibitor concentration is increased, the potential range of the second anodic peaks shifts from negative to positive, and the peaks progressively fade. The results show that the plant extract is an efficient mild steel inhibitor.

Bode Measurements: Figure 7 depicts a resistive zone at high frequencies and a capacitive region at intermediate frequencies, but no distinct resistive region (horizontal line and phase angle of 0°) at low frequencies. At low frequencies, these graphs show two phase maxima that overlap. The impedance is shown on the X axis with log frequencies on the X axis and the log of the absolute value of the impedance and phase shift on the Y axis in the bode plot. The phase angle does not exceed 90 degrees, as it would for pure capacitive impedance, as it does in the Nyquist figure. Log (Rs + Rct) shows as a horizontal plateau in the bode plot at the highest frequencies.

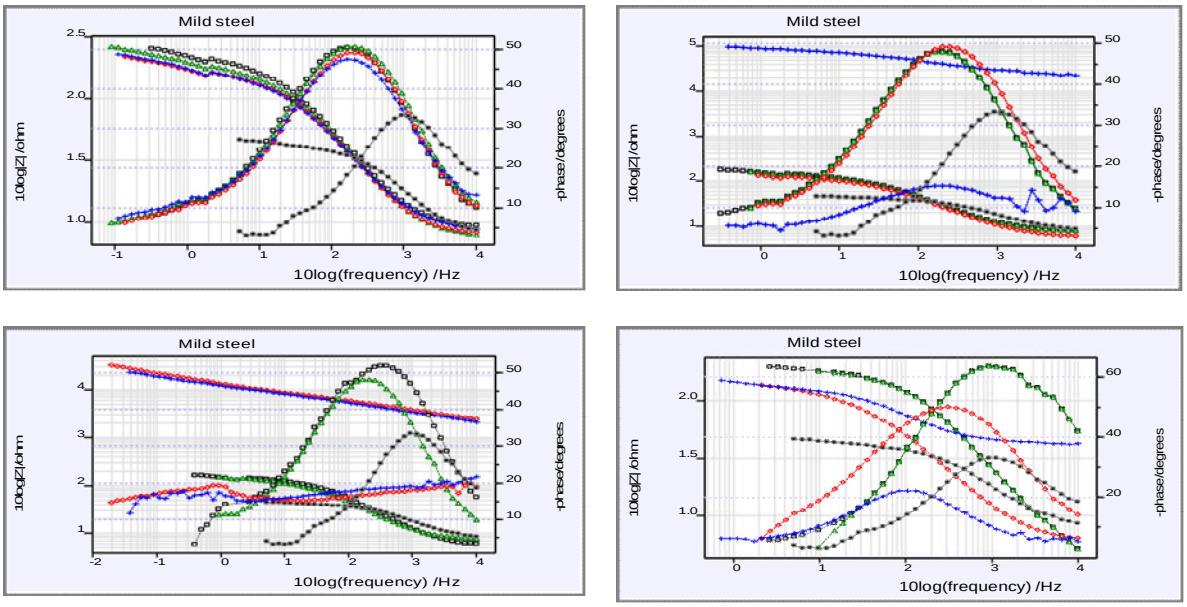

Figure 7. Bode plots of mild steel in alcoholic solution.

Adsorption studies: In terms of inhibitor adsorption properties, the nature of inhibitor interaction on the corroding surface during metal corrosion inhibition has been determined. The ether adsorption of the plant components of a barrier film separating the metal surface from the corrosive medium is attributed to the decrease in corrosion rate caused by the addition of alcoholic extract of GSL plant, and this is usually confirmed by fitting the experimental data to various adsorption isotherms. The nature and surface charge of the metal, the kind of aggressive electrolyte, and the chemical structure of inhibitors all impact the adsorption process.It was discovered that the adsorption of GSL plants conform to different isotherms, including Frumkin, Langmuir, Temkin, Hasley, Freundlich, and Flory-Huggins. Surface coverage (**θ**) was plotted versus Ln C in figure 8-10 for the Temkin, Hasley and Langmuir isotherm. R^2 is nearly equal to 1 for a straight line with a regression coefficient. Concentration inhibitor molecules begin to desorb as corrosion inhibitor concentration increases owing to interactions between inhibitory molecules already adsorbed at the surface and those present in the solution. The connection becomes stronger as the inhibitor level rises.

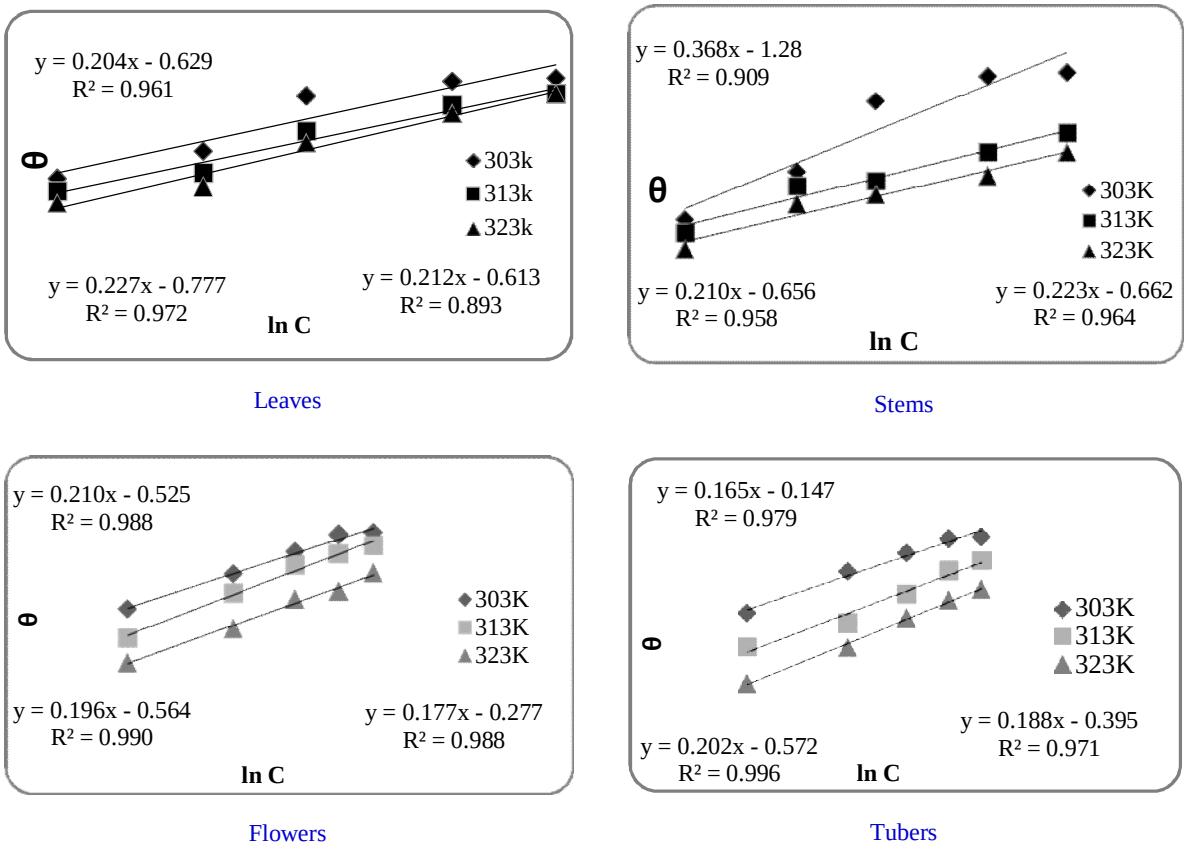

Figure 8. Temkin adsorption isotherm plot for mild steel in 1N HCl containing different concentration of Gloriosa superb linn plant alcoholic extracts (a) leaves (b) stems (c) flowers and (d) tubers.

Phytochemical screening method: The existence of several chemical constituents such as alkaloids, carbohydrates, proteins, saponins, triterpinoids, and tannins was examined using phytochemical screening of the aerial sections of the plant's powder alcoholic extract, and the results are presented in Table 6. As a consequence, the metal's corrosion rate was reduced. The development of a film layer effectively prevents H+ discharge and metal ion dissolution. The protonated constituent's molecules are adsorbed (physisorption) due to electrostatic contact, and significant inhibition is predicted.

GC-MS Technique: Figure 11 shows the spectra of crude plant extract obtained by gas chromatography and mass spectroscopy. The GC-MS analysis quantitatively identified every organic species. Each chromatogram peak's size was proportional to the number of organic molecules that

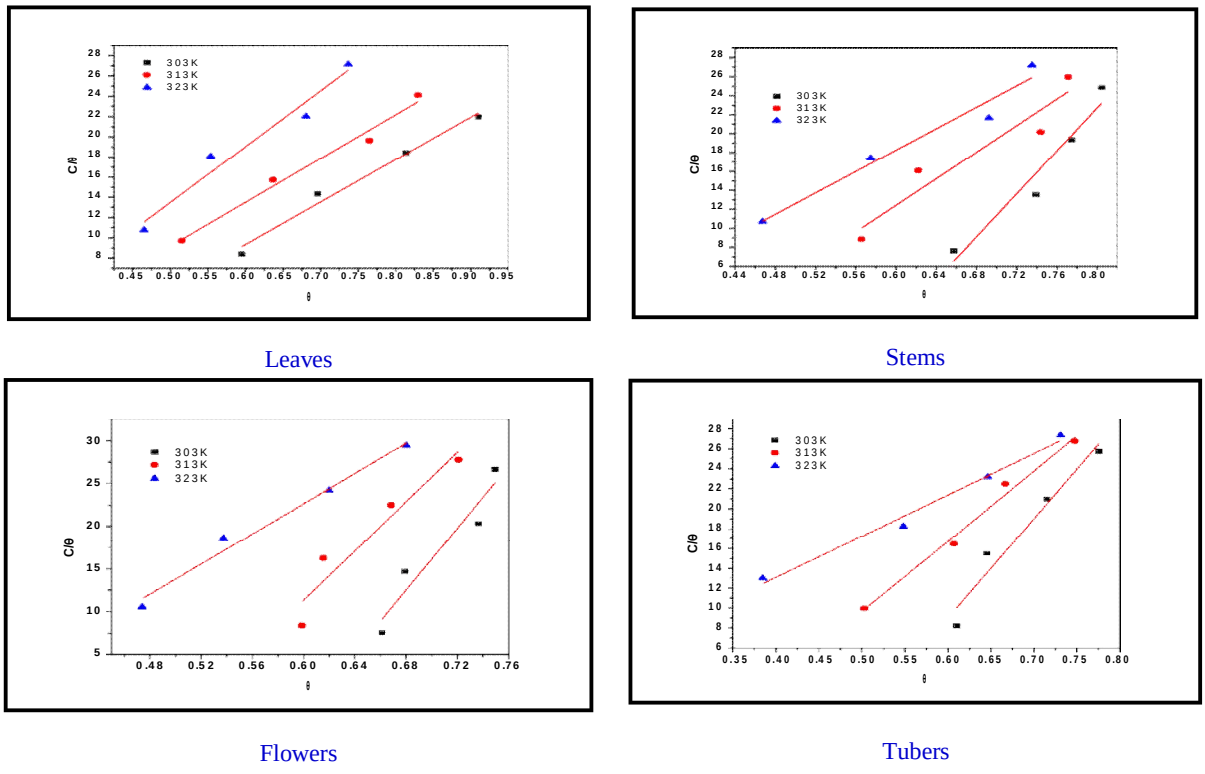

Figure 9. Langmuir adsorption isotherm plot for mild steel in 1N HCl containing different concentration of *Gloriosa superba linn* plant alcoholic extracts (a) leaves (b) stems (c) flowers and (d) tubers.

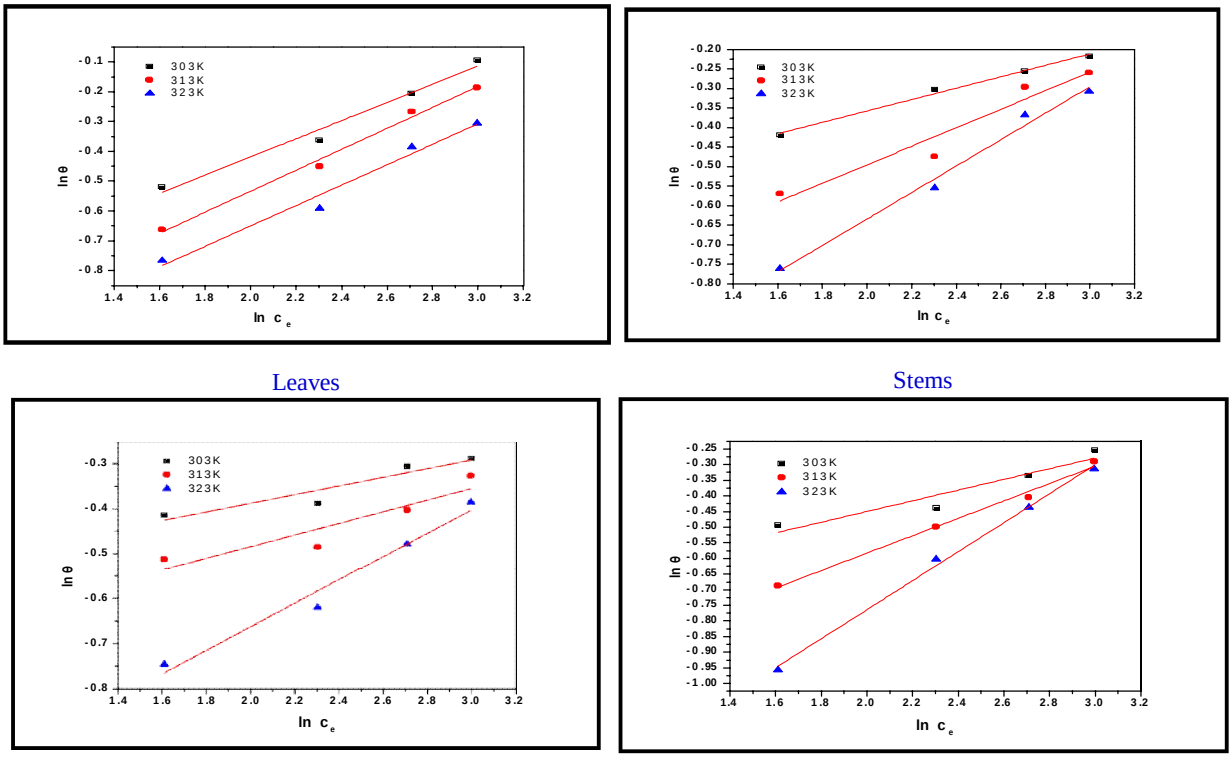

Figure 10. Hasley adsorption isotherm plot for mild steel in 1N HCl containing different concentration of *Gloriosa superb linn* plant alcoholic extracts (a) leaves (b) stems (c) flowers and (d) tubers.

Table 6. Phytochemical screening test of extract of *Gloriosa Superba* Linnm**(GSL)** plant

Alcoholic extract				
Phytochemical test	**Leaves**	**Stem**	**Flowers**	**Tubers**
Alkaloids	+	+	+	+
Carbohydrates	-	-	-	+
Proteins	+	+	+	+
Saponins	-	+	+	-
Thiols	-	-	-	-
Tannins	+	-	+	+
Flavanoids	+	+	+	+
Phenol	-	-	-	-
Glycosides	-	-	+	-

(+).. Presence (-)... Absence

formed that peak. The structural attribution of the compound's GC retention data is based on spectrum matching with the literature. The GSL is made up of five main components, as can be seen. Because the majority of chemicals has similar retention times and is difficult to distinguish, the GSL plant extract was utilized for corrosion inhibition investigations. The structure of the following component comprises electron-rich oxygen and nitrogen, which might be useful active components for plant corrosion inhibition.

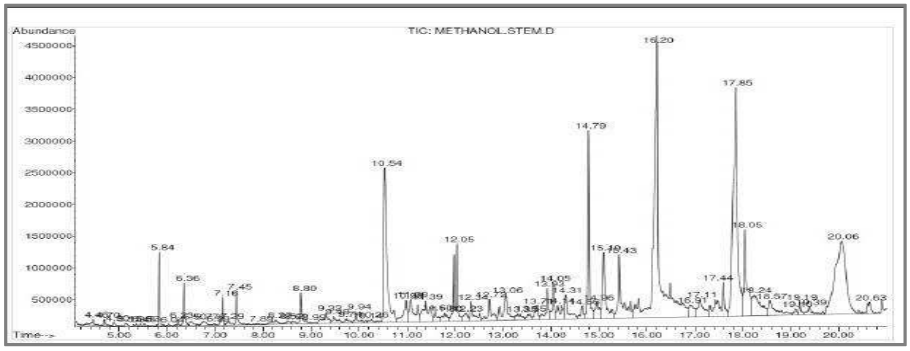

Figure 11. The GC-MS combines the gas chromatography and mass spectrometry techniques.

These components clearly have bi bonds and heteroatoms, as seen in the figure of constituents (oxygen). As a result, either the electrostatic contact of charged molecules with inhibitor ingredients or the interaction of unshared electrons in inhibitor molecules causes adsorption. The direct interaction of the lone pairs of electrons on O and N with the unoccupied d-orbitals of Fe can cause adsorption of protonated molecules in the plants extract on the mild steel surface. Metal inhibitor complexes with Fe^{2+} ions generated during anodic breakdown of steel might also provide this loan pair of electrons. Through van der Waals force, these complexes may adsorb onto the steel surface, giving further corrosion protection.

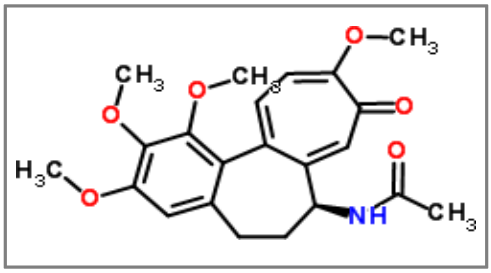

Figure 12. Chemical structure of Colchicine

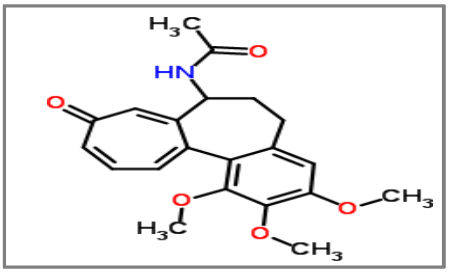

Figure 13. Chemical structure of Colchides

CONCLUSION

In 1 N HCl acid, Gloriosa superba plants are an effective corrosion pickling inhibitor on mild steel. *Gloriosa superba* plants were used as a corrosion inhibitor since they were ecologically acceptable, non-toxic, cost effective, and readily available. *Gloriosa superba* plant extracts had a maximum effectiveness of 94.12 percent leaves for a one-day immersion duration at room temperature at the optimal concentration of 20 v/v. The results of non-electrochemical methods (weight loss method) are quite similar to those of electrochemical methods. On the metal surface, the extracts of *Gloriosa superba* plants operate as a mixed type inhibitor. SEM analysis revealed that the surface morphology of the as corroded inhibited mild steel samples was improved as compared to uncontrolled samples.

REFERENCES

[1]. K. Vinothkumar, M. Nivetha, M.G Sethuraman, *Iran Polym J*, **2020**, 29, 919-931.
[2]. Z. Hamidi, S.Y Mosavian, N. Sabbaghi, *Iran Polym J*, **2020**, 29, 225-239.
[3]. M. EPekdemir, E. Öner, M. Kök , *Iran Polym J*, **2021**, 30, 633-641.
[4]. O. Dagdag, A. El Harfi, L. El Gana, Z. Hlimi, H. Erramli, O. Hamed, S. Jodeh, *J Bio-Tribo-Corros*, **2019**, 5(1), 7-16.
[5]. R. Huang, X. Guo, S. Ma, J. Xie, J. Xu,J. Ma, *Polymers*, **2020**, 12(1), 108-120.
[6]. O. Dagdag, R.Hsissou, A. Berisha, H.Erramli, O. Hamed, S.Jodeh, A. El Harfi, *J Bio-Tribo-Corros*, 2019, 5, 58-64.
[7]. L. Li, Z. Cai, *Polymers*, **2020**, 12, 317-324.
[8]. K. Song, Y. Wang, F. Ruan, J. Liu, N. Li, X. Li, *Polymers*, **2020**, 12, 132-140.
[9]. A.V. Rane, V. Abitha, S. Jadhava, *Moroc J Chem.*, **2020**, 8, 8-4.
[10]. R.Kanojia, G.Singh, Surface Eng, **2005**, 21(3), 180-186.
[11]. Li W, He Q, S. Zhang, C. Pei, B.J Hou, Appl Electrochem, **2008**, 38, 289-295.
[12]. P. R. Sivakumar, A. P . Srikanth, *Int J. Phy Appli Sci.*, **2016**, 3(1), 10-20.
[13]. P. R. Sivakumar, M.Karuppusamy, S. Perumal, A. Elangovan, A.P Srikanth, *J Envi Nanotech*, **2015**, 4(2), 31-36.
[14]. M. Karuppusamy, P. R. Sivakumar, S. Perumal, A. Elangovan, A.P Srikanth, *J Envi Nanotech*, **2015**, 4(2), 09-15.
[15]. P. R. Sivakumar, A. P. Srikanth, *Int J Eng Sci and Comp*, **2016**, 6(8), 2744-2748.
[16]. P. R. Sivakumar, M. Karuppusamy, K.Vishalakshi, A. P. Srikanth, *Der Pharma Chemi*, **2016**, 8(12), 74-83.
[17]. P. R. Sivakumar, K. Vishalakshi, A.P Srikanth, J Appli Chemi, **2016**, 5(5), 1080-1088.
[18]. K. Vishalakshi, P. R Sivakumar, A. P. Srikanth, *J Appli. Chemi*, **2016,** 9(9), 50-55.
[19]. P. R. Sivakumar, A.P Srikanth,*Int Org Sci Res J Appli. Chemis*, **2016**, 369(10), 29-37.
[20]. P. R. Sivakumar, A. P Srikanth, *Der Phar Chemi*, **2016**, 8(19), 433-440.
[21]. P. R. Sivakumar, M. Karuppusamy, K. Vishalakshi, A.P. Srikanth, *IOSRD Int J Chemi*, **2017**, 4(1), 14-18.
[22]. P. R. Sivakumar, A.P. Srikanth, *Asian J Chemi*, **2017**, 29(2), 274-278.
[23]. K. Vishalakshi, P. R. Sivakumar, A.P Srikanth, *Der Pharma Chem*, **2016**, 8(19), 548-553.
[24]. Akil khajuria, Modassir Akhtar, Raman Bedi, Rajneesh Kumar, Mainak Ghosh, Das CR, Shaju K Albert, *Mat Sci and Tech*, **2020**, http://doi.org/10.1080/02670836.2020.1784543.
[25]. Akil khajuria, Modassir Akhtar, Raman Bedi, Rajneesh Kumar, Mainak Ghosh, Das CR, Shaju K Albert, *Int.J. Pressure ves pip*, **2020**, http://doi.org/10.1016/j.ijpvp.2020.104246.
[26]. Akil khajuria, Modassir Akhtar, Raman Bedi, Rajneesh Kumar, Mainak Ghosh, Das CR, Shaju K Albert, *App. Nanoscience*, **2018**, http://doi.org/10.1007/s13204-018-0854-1.
[27]. P. R. Sivakumar, A. P Srikanth, *J Appli. Chem.*, **2017**, 6(4), 476-483.
[28]. P. R. Sivakumar**,** A.P Srikanth, *J Appli. Chem.*, **2018**, 7(1), 239-249.
[29]. P. R. Sivakumar, A.P Srikanth, *Asi J Chemis*, **2018**, 30(3), 513-519.
[30]. P. R. Sivakumar, A.P Srikanth, S. Muthumanikam, *Int J Chemtech Res*, **2017**, 10(12), 386-398.
[31]. P. R. Sivakumar, M.Karuppusamy, A.P Srikanth, *Int Org Sci Res J Appl Chem.*, **2017**, 10, 65-70.

[32]. P. R. Sivakumar, M.Karuppusamy, A.P Srikanth, *Der Phar Chemi*, **2018**, 10:22-28.
[33]. P. R. Sivakumar, A.P Srikanth, *Sadhana* , **2020**, 45, 45-56.